JOURNAL OF GEOPHYSICAL RESEARCH, VOL. 108, NO. D4, 8251, doi:10.1029/2001JD000866, 2003

Hydrocarbon measurements at Pabstthum during the BERLIOZ campaign and modeling of free radicals

S. Konrad,[1] Th. Schmitz,[2] H.-J. Buers, N. Houben, K. Mannschreck,[3] D. Mihelcic, P. Müsgen, H.-W. Pätz, F. Holland, A. Hofzumahaus, H.-J. Schäfer,[4] S. Schröder, and A. Volz-Thomas

Institut für Chemie und Dynamik der Geosphäre II, Forschungszentrum Jülich, Jülich, Germany

K. Bächmann and S. Schlomski

Fachbereich 7: Chemie, Technische Hochschule Darmstadt, Darmstadt, Germany

G. Moortgat and D. Großmann

Division of Atmospheric Chemistry, Max-Planck-Institut für Chemie, Mainz, Germany

Received 22 May 2001; revised 21 November 2001; accepted 17 December 2001; published 29 January 2003.

[1] The Photochemistry Experiment in BERLIOZ (PHOEBE) was conducted in July/August 1998 at a rural site located near the small village Pabstthum, about 50 km NW of downtown Berlin. More than 60 nonmethane hydrocarbons (NMHC) in the range of C_2-C_{10} were measured using two in situ gas chromatography (GC) systems. The first (GC1) was capable of measuring C_2-C_{10} hydrocarbons with a relatively high separation efficiency but low time resolution (80–90 min), while GC2 provided quasi-continuous measurements of C_5-C_{10} hydrocarbons with a time resolution of 20 min but with a poorer separation efficiency than GC1. The advantages of both systems were joined by interpolation between two data points of GC1 with the pattern given by GC2. For compounds that could not be reliably measured with GC2, patterns of compounds with similar reactivity were used. Air masses with the lowest photochemical age as estimated from the toluene/benzene ratio and the highest hydrocarbon mixing ratios were observed on 20 and 21 July when air was advected from the direction of Berlin. Alkanes were the most abundant hydrocarbons (~60%) on a molecular basis, followed by alkenes and aromatics. The reactivity of the hydrocarbons toward OH was dominated by the alkenes (>60%), with isoprene and α-pinene constituting the major part. The hydrocarbon data were used together with the other trace gases measured at Pabstthum to simulate OH, HO_2, and RO_2 concentrations with the condensed chemical box model RACM. Relatively good agreement of the simulated radical concentrations with the spectroscopic measurements made at Pabstthum is observed for NO_x mixing ratios >5 ppb, whereas the model overestimates OH and HO_2 by 100% and 40%, respectively, at low NO_x. The discrepancy between measured and modeled OH does not correlate with the concentration of particles. The RO_2 concentrations are in good agreement with the measurements over the entire range of NO_x. Sensitivity studies show that peroxyacetyl nitrate (PAN) is an important radical source and that missing volatile organic compound (VOC) reactivity is an unlikely explanation for the overestimation of HO_x: By doubling of the VOC reactivity, OH and HO_2 can be brought into agreement. However, the model then overestimates the organic RO_2 concentrations by almost a factor of 2. Another important finding is that RACM overestimates the measured NO/NO_2 ratio by 25%. This and the overestimation of HO_2 lead to an overprediction of the local ozone formation rate by about 40% at low NO_x mixing ratios. *INDEX TERMS:* 0365 Atmospheric Composition and Structure: Troposphere—composition and chemistry; 0345 Atmospheric Composition and Structure: Pollution—urban and regional (0305); 0322 Atmospheric Composition and Structure: Constituent sources and sinks; *KEYWORDS:* hydrocarbons, gas chromatography, free radicals, field measurements, chemical mechanism, modeling

[1]Now at Bayer AG, Dormagen, Germany.
[2]Now at Engelhard Technologies, Hannover, Germany.
[3]Now at Deutscher Wetterdienst, Meteorologisches Observatorium, Hohenpeißenberg, Germany.
[4]Now at FJA-innosoft GmbH, Köln, Germany.

0148-0227/03/2001JD000866

Citation: Konrad, S., et al., Hydrocarbon measurements at Pabstthum during the BERLIOZ campaign and modeling of free radicals, *J. Geophys. Res.*, *108*(D4), 8251, doi:10.1029/2001JD000866, 2003.

1. Introduction

[2] Volatile organic compounds (VOC) play an important role in the formation of photo oxidants such as ozone, peroxyacetyl nitrates (PANs) and peroxides and influence the recycling of free radicals. Accurate measurements of VOC are thus a prerequisite in field experiments that address the budget of radicals and photo oxidants. Because of their short chemical lifetimes between 1 and 100 s during daytime, free radicals (OH, HO_2, and RO_2) are largely decoupled from transport processes and can thus be investigated with zero dimensional chemistry models, provided that the chemical and physical parameters which control the local radical concentration, e.g., UV radiation, NO_x, and VOC, are quantified. This is strictly the case only if the radicals and other parameters are measured with a time resolution given by the atmospheric lifetimes of the radicals, e.g., between less than 1 s for OH and a few seconds to minutes for the peroxy radicals. Until now this is an unsolved challenge for many atmospheric trace gases, in particular for hydrocarbons which in urban air can constitute of more than 100 different compounds [*Ciccioli et al.*, 1992]. Besides time resolution, representativeness and sufficient separation of the complex hydrocarbon mixture is necessary for a quantitative understanding of their influence on the radical chemistry. The latter requirement limits at present to some extent the applicability of proton transfer mass spectrometry [*Lindinger et al.*, 1998], which is extremely fast ($\sim$1 s) but provides reliable information only for a limited range of atmospheric VOCs.

[3] HC measurements are usually made by gas chromatography (GC), either off-line on samples collected in special canisters [e.g., *Blake et al.*, 1993; *Greenberg et al.*, 1992, 1996; *Habram et al.*, 1998; *Rudolph*, 1995; *Rudolph et al.*, 1990b] or on adsorption tubes [*Ciccioli et al.*, 1992; *Grob and Grob*, 1971; *Knobloch et al.*, 1997] or by deploying in situ GC systems in the field [e.g., *Helmig and Greenberg*, 1994; *Kramp and Volz-Thomas*, 1997; *Rudolph et al.*, 1990a; *Wedel et al.*, 1998]. Most measurements reported in the literature are made with relatively long columns in order to achieve the required separation efficiency, resulting in analysis times of 1 hour or more. While this conflicting situation can principally be resolved by off-line sampling, the amount of containers or adsorption tubes needed for large field experiments and the necessary tests for sample integrity place extreme logistic demands.

[4] In the past several campaigns were conducted in order to investigate the fast photo chemistry by measurements of the concentrations of the free radicals (OH, HO_2, and RO_2) and of those chemical and physical parameters that are thought to control the radical concentrations [cf. *Perner et al.*, 1987; *Poppe et al.*, 1994; *Eisele et al.*, 1994, 1996, 1997; *Cantrell et al.*, 1996, 1997; *Carpenter et al.*, 1997; *Penkett et al.*, 1997; *Mount and Williams*, 1997; *McKeen et al.*, 1997; *Brandenburger et al.*, 1998; *Holland et al.*, 1998; *Hauglustaine et al.*, 1999; *Ehhalt*, 1999; *Carslaw et al.*, 2000a, 2000b; *Volz-Thomas and Kolahgar*, 2000; *Brauers et al.*, 2001; *Savage et al.*, 2001]. Although the comparison of measurements and models does not show a coherent picture, there is a general tendency of photochemical models to overestimate OH and peroxy radicals. Exceptions are, e.g., the ALBATROSS and POCORN campaigns, and the MLOPEX-2 campaign in spring, where modeled and measured OH were found to agree within the experimental uncertainties [*Brauers et al.*, 2001; *Ehhalt*, 1999; *Eisele et al.*, 1996], and the SLOPE campaign, where OH was found to be significantly underestimated by the model [*Volz-Thomas and Kolahgar*, 2000]. In some studies, the comparison was somewhat limited by the lack of measurements for several trace gases that are of importance to OH formation or loss, e.g., part of the VOC.

[5] The Photochemistry Experiment in BERLIOZ (PHOEBE) was conducted in summer 1998 as part of the BERLIOZ campaign [*Becker et al.*, 1999] in order to investigate the fast photochemistry in an urban/suburban environment. An overview of the general objectives and activities is given by *Volz-Thomas et al.* [2003a]. In this paper we report measurements of C_2-C_{10} hydrocarbons by joining the advantages of two different in situ GCs, one with a relatively high separation efficiency but low time resolution (80–90 min) and the other with a lower separation efficiency providing quasi continuous measurements of C_5-C_{10} hydrocarbons with a time resolution of 20 min. The hydrocarbon data are used in connection with the other trace gas measurements made at Pabstthum [*Grossmann et al.*, 2003; *Volz-Thomas et al.*, 2003b] to evaluate the photochemical box model RACM by comparing the simulated OH, HO_2 and RO_2 concentrations with the measurements by LIF [*Holland et al.*, 2003] and MIESR [*Mihelcic et al.*, 2003].

2. Experimental

[6] The measurements were conducted near the small village Pabstthum about 50 km NW from the city center of Berlin. A description of the site and a summary of the chemical and meteorological measurements are given in the work of *Volz-Thomas et al.* [2003a] and in the other papers of this special section. The nonmethane hydrocarbons (NMHC) were determined by in situ GC with two different systems, namely an Airmotec HC1010 and a custom made system built around a HP5890 (referred to as HP-GC). The experimental setup and an evaluation of the analytical systems is presented elsewhere [*Konrad and Volz-Thomas*, 2000; *Schmitz et al.*, 1997, 2000]. Therefore, only a brief summary of the most important features is presented here.

[7] The HC1010 is appropriate for measuring C_5-C_{10} HC with a sampling interval of 19 min and a time resolution of 20 min. Samples are collected on adsorption tubes containing Carbotrap and Carbosieve SIII (3:1, Supelco, Bellefonte, PA, USA) at ambient temperature. After refocusing on a micro packed capillary column (O.D. = 0.78 mm, I.D. = 0.50 mm, l = 18 cm, 5 cm packing of Carbopack B, Supelco) the hydrocarbons are injected and separated on a 9.5 m DB-5 capillary column (J&W Scientific, Folsom, CA, USA, 250 μm I.D., 1 μm film, temperature program: 1 min at 30°C, from 30 to 140°C at 10°C min^{-1}, 1 min at

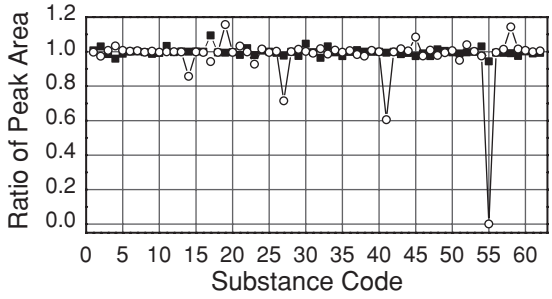

Figure 1. Test of the inlet line and ozone scrubber used during BERLIOZ with the NCAR-BERLIOZ standard. Shown is the ratio of the peak areas obtained through the original 11 m long inlet line to the peak areas obtained with a new short silco steel tube as a function of the mixing ratio of the compounds (filled triangles: O_3 scrubber in the long inlet line; open circles: without O_3 scrubber). Compound numbers: 1: ethene, 2: ethyne, 3: ethane, 4: propene, 5: propane, 6: 2-methylpropane, 7: 1-butene, 8: n-butane, 9: trans-2-butene, 10: cis-2-butene, 11: 3-methyl-1-butene, 12: 2-methylbutane, 13: 1-pentene, 14: 2-methyl-1-butene, 15: n-pentane, 16: 2-methyl-1,3-butadiene, 17: trans-2-pentene, 18: cis-2-pentene, 19: 2-methyl-2-butene, 20: 2,2-dimethylbutane, 21: cyclopentene, 22: 4- and 3-methyl-1-pentene, 23: cyclopentane, 24: 2, 3-dimethylbutane, 25: 2-methylpentane, 26: 3-methylpentane, 27: 2-methyl-1-pentene, 28: n-hexane, 29: cis-3-hexene, 30: trans-2-hexene, 31: cis-2-hexene, 32: methylcyclopentane, 33: 2, 4-dimethylpentane, 34: benzene, 35: cyclohexane, 36: 2-methylhexane, 37: 2, 3-dimethylpentane, 38: 3-methylhexane, 39: 2, 2, 4-trimethylpentane, 40: n-heptane, 41: 2, 3-dimethyl-2-pentene, 42: methylcyclohexane, 43: 2, 3, 4-trimethylpentane, 44: toluene, 45: 2-methylheptane, 46: 4-methylheptane, 47: 3-methylheptane, 48: n-octane, 49: ethylbenzene, 50: m/p-xylene, 51: styrene, 52: o-xylene, 53: n-nonane, 54: i-propylbenzene, 55: α-pinene, 56: n-propylbenzene, 57: m-ethyltoluene, 58: p-ethyltoluene, 59: 1, 3, 5-trimethylbenzene, 60: o-ethyltoluene, 61: 1, 2, 4-trimethylbenzene, 62: n-decane.

140°C). Detection limits range from 1 to 8 ppt. Due to its high time resolution and its quasi continuos measuring cycle the HC1010 suffers from coelution especially with oxygenated compounds as identified by *Konrad and Volz-Thomas* [2000].

[8] The HP-GC is suitable for the detection of C_2-C_{10} HC. The hydrocarbons identified on the HP-GC are displayed in Figure 1. Sampling is done cryogenically for 20 min at the end of a 80–90 min measuring cycle. Separation is achieved on a 90 m DB-1 capillary column (320 μm ID, 3 μm film, temperature program: 2 min at −50°C, −50° to 200°C at 5°C min^{-1}, 15 min at 200°C). Detection limits range from 20 to 4 ppt (ethene: ~80 ppt due to CO_2 interference). Because of the much better separation efficiency, coelution is negligible for most compounds [*Schmitz et al.*, 2000].

[9] Absolute calibration of both systems was based on a custom-made diffusion source which was compared during BERLIOZ to a certified 70 component standard (referred to as NCAR-BERLIOZ standard [*Volz-Thomas et al.*, 2002]). Averaged over all compounds, the systematic deviation between our own calibration and the NCAR certificate was −3% with a standard deviation of 6%, in good agreement with the estimated accuracy of the diffusion source [*Konrad and Volz-Thomas*, 2000]. In ambient air, good agreement between the HC1010 and the HP-GC (2σ deviation <14% or <10 ppt) was found for HCs and groups of HCs that are free from coelution with oxygenated compounds, whereas large discrepancies (in some cases more than a factor of 3) were found for those HCs that coelute with oxygenated compounds on the HC1010 [*Konrad and Volz-Thomas*, 2000].

[10] A 11 m long 1/8 inch O.D. Silco Steel tube (Restek) heated to 50°C, which had been used before during several campaigns [*Kramp and Volz-Thomas*, 1997; *Volz-Thomas and Kolahgar*, 2000], was used for sampling. The inlet was located about 10 m above ground on a pneumatic mast. Ambient ozone has been identified as a potential interference with the measurement of alkenes, in particular if large concentrations are accumulated during preconcentration. The different ozone scrubbers described in the literature were reviewed by *Helmig* [1997]. It was noted that some of the scrubbers, besides removing ozone, may also interact themselves with the reactive hydrocarbons in the sample, thus not always leading to the wanted improvement in the alkene measurement. We used a 2 m section of 1/8 in. O.D. stainless steel tubing, heated to 90°C, as an O_3 scrubber [*Koppmann et al.*, 1995; *Schmitz et al.*, 1997]. Tests of the scrubber before the campaign with an alkene standard demonstrated that losses of ethene, propene, 1-butene and 1-hexene were <10% in the presence of 110 ppb O_3 [*Konrad and Volz-Thomas*, 2000].

[11] After BERLIOZ, a test of the entire inlet system was performed at FZ-Jülich. First, the NCAR-BERLIOZ standard was alternatively injected into the HP-GC through the 11 m long Silco Steel inlet line and through a new 1 m long Silco Steel tube. These tests were made without the O_3 scrubber in place. The inlet line was in the condition as at the end of BERLIOZ and no cleaning was applied before the experiments. Subsequent tests were made with the original O_3 scrubber installed between the long inlet line and the GC.

[12] The results of both tests are displayed in Figure 1. Without O_3 scrubber, the ratio of the peak areas obtained with the two inlets is 1.00 ± 0.025 (1σ) without any systematic differences for the higher boiling compounds or for groups of hydrocarbons. With the O_3 scrubber in place, the situation is equally good except for the alkenes. Significant losses are observed for 2-methyl-1-butene, 2-methyl-1-pentene, 2, 3-dimethyl-pentene and, in particular, α-pinene. The losses of 2-methyl-1-butene in the scrubber are compensated within a few percent by an increase in 2-methyl-2-butene. Additional peaks of a (yet unidentified) C_6 alkene and an unidentified terpene in the chromatogram of the HP-GC account for approximately 80% of the decline of 2-methyl-1-pentene and α-pinene, respectively. It seems therefore most probable that the apparent losses of the above mentioned alkenes in the ozone scrubber are due to isomerization. Only in case of 2, 3-dimethylpentene, there are no additional peaks detected that would compensate for the decline. However, this substance was always below the detection limit during the BERLIOZ campaign.

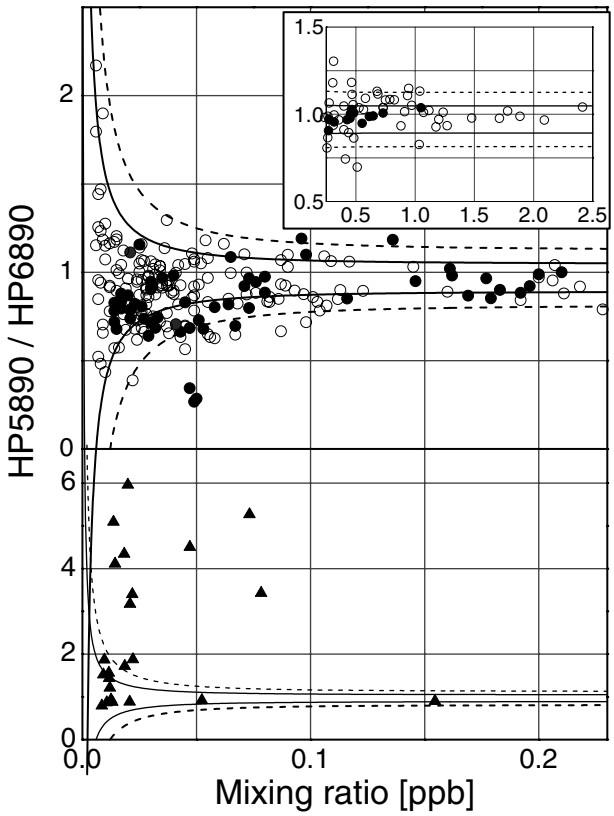

Figure 2. Ratios of the HC concentrations determined with the HP5890 with the BERLIOZ inlet line to those determined with the HP6890 with a short new inlet line as a function of the actual mixing ratios in ambient air. Upper panel: alkanes (open circles), aromatics, and ethyne (filed circles). Lower panel: alkenes (triangles). The solid (1σ) and dashed (2σ) lines, which embrace the middle 68% and 90% of the data in the upper panel, respectively, are calculated with bias of 3%, a relative error of 8% and an absolute error of 6 ppt.

[13] We should like to emphasize that isomerization was not observed when the NCAR-BERLIOZ standard was measured at the beginning of the BERLIOZ campaign. On 19 July all alkenes including α-pinene agreed within 20% or better with the certified values. At the end of the campaign, on 4 August α-pinene losses of ∼50% were determined. The ambient α-pinene values measured during BERLIOZ could therefore be underestimated by as much as 50%.

[14] Additional tests of the BERLIOZ inlet line (and O_3 scrubber) were performed in ambient air by using two almost identical HP-GC systems. The GC used during PHOEBE (HP5890 = HP-GC) sampled through the long inlet line and O_3 scrubber, whereas the other GC (HP6890) had a short inlet line of ∼1 m [*Konrad and Volz-Thomas*, 2000]. Both systems were harmonized by calibration with the same reference mixture. The analytical cycles were synchronized as far as possible.

[15] Figure 2 shows the ratios of the concentrations as determined with the two inlets as a function of the mixing ratios measured with the short inlet. The scatter in the upper panel can be best described by a bias of 3%, a relative error of 8% and an absolute error of 6 ppt (dashed lines = 1σ; dotted lines = 2σ). The relative and absolute errors are similar to those observed for the comparison of the HC1010 and HP-GC at Pabstthum as described above. No systematic differences between alkanes and aromatics are observed (upper panel). The barely significant bias of 3% is most likely due to unresolved differences in calibration between the two GCs and small differences in timing, rather than a result of losses in the long inlet line. As can be seen from the lower panel of Figure 2 alkenes are underestimated by the HP6890 up to a factor of 6. This is most probably due to the absence of an O_3 scrubber in front of the HP6890.

3. Results

[16] Figure 3 shows the hydrocarbon mixing ratios as measured during BERLIOZ with the HP-GC The lowest panel gives the sum of the mixing ratios of all measured compounds (including isoprene and α-pinene). The most abundant individual compounds are shown in the upper

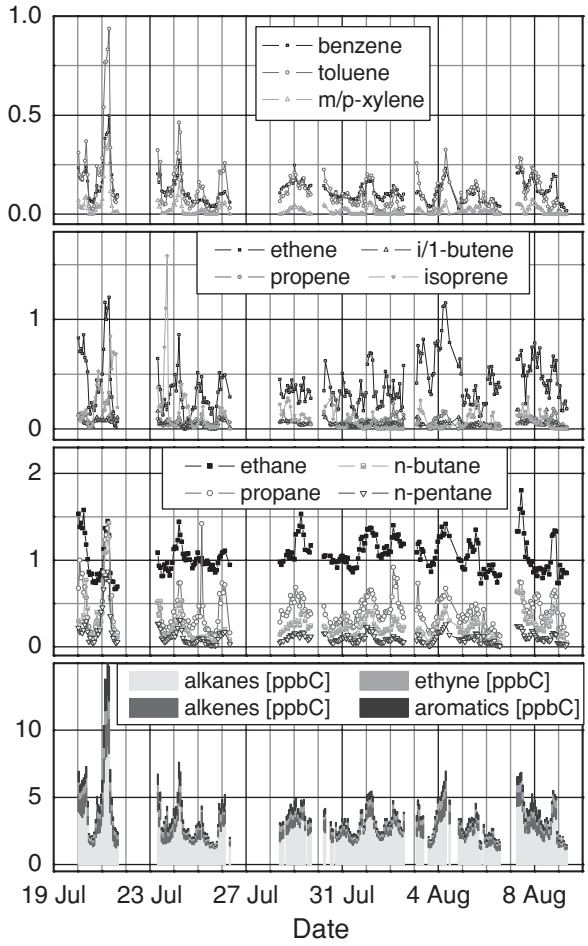

Figure 3. Time series of selected hydrocarbons as measured with the HP-GC at Pabstthum during BERLIOZ. The lowest panel shows the sum of all identified compounds and the breakdown into classes. The upper panels show the most abundant compounds of each hydrocarbon class. See color version of this figure at back of this issue.

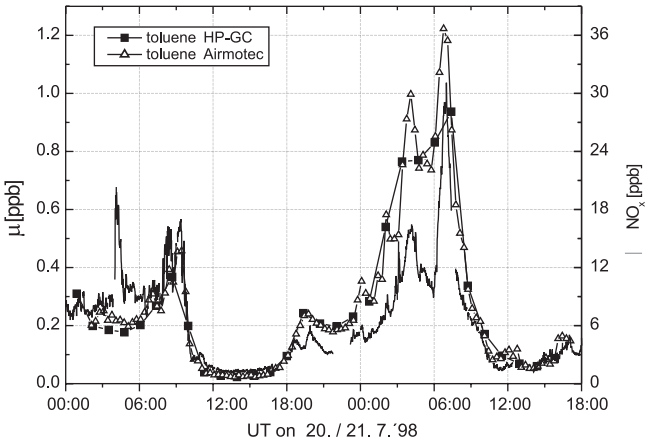

Figure 4. Time series of toluene measured with the HP-GC (squares) and the HC1010 (triangles) and NO_x (solid line, right ordinate) at Pabstthum during the first IOP (20 and 21 July).

panels. On the basis of the measured mixing ratios, alkanes make the largest contribution (50% or more) to the sum of all hydrocarbons during the whole campaign followed by the alkenes (in particular isoprene) and aromatics. Generally, lower concentrations are observed during daytime while the highest concentrations are found during night and in the early morning. This behavior can be principally explained from the diurnal variation of the hydroxyl radical concentrations with a maximum around local noon [*Holland et al.*, 2003] and the build up of a shallow surface inversion with low wind speeds at night [*Glaser et al.*, 2003].

[17] The highest mixing ratios of all compounds with anthropogenic sources were observed on 20 and 21 July during the first intensive observational period (IOP) when the wind came from the direction of Berlin. Figure 4 gives a closer look on the diurnal variation of the toluene mixing ratios measured with the HP-GC and the Airmotec HC1010 during the first IOP. To identify polluted air masses the NO_x mixing ratios of *Volz-Thomas et al.* [2003b] are depicted on the right ordinate. The diurnal variation of the toluene mixing ratio follows the diurnal variation of NO_x. The maxima of both, NO_x and toluene coincide in the morning hours of both days. For the further discussion we refer to the time periods with elevated NO_x mixing ratios around 09 UT on 20 July and around 07 UT on 21 July as "plume" events. Figure 4 emphasizes the importance of highly time resolved hydrocarbon measurements: The measurements made with the HP GC due to its long analytical cycle miss the concentration maximum in the time series on 21 July. A linear interpolation of the HP-GC data would lead to a significant underestimation of the hydrocarbon concentration and hence the VOC/NO_x ratio in the plume which is of particular interests for the free radicals and ozone formation [*Trainer et al.*, 1987].

3.1. Combination of the Two Hydrocarbon Data Sets

[18] Since the HC1010 measures only a limited number of compounds with sufficient accuracy [*Konrad and Volz-Thomas*, 2000] the data sets from both GC systems were combined to join the high time resolution of the HC1010 with the high precision and the larger number of measurable compounds on the HP-GC, which had been selected as the reference instrument for the BERLIOZ campaign [*Volz-Thomas et al.*, 2002].

[19] For compounds where good agreement between the HC1010 and the HP-GC was observed in ambient air (class A compounds) [cf. *Konrad and Volz-Thomas*, 2000], the values determined with the HC1010 were corrected with the results from a linear regression between the HC1010 and the HP-GC. The correction was generally <5%, since both GCs had been calibrated with the same hydrocarbon standards. Peaks consisting of more than one hydrocarbon (e.g., benzene + cyclohexane) were subsequently separated using the ratio determined by the HP-GC.

[20] For hydrocarbons $<C_5$ and those suffering from coelution with oxygenated compounds on the HC1010 (class B compounds), the concentrations were interpolated between two data points of the HP-GC using the pattern of a proxy hydrocarbon of similar reactivity toward OH obtained with the HC1010. The procedure implies the assumption that both hydrocarbons A and B have a similar source distribution. The hydrocarbons from class B and the hydrocarbons from class A that were used for the interpolation are listed in Table 1. The right column of Table 1 gives the correlation coefficients between hydrocarbons A and B. For most pairs, the correlation is relatively tight ($R^2 > 0.8$)

Table 1. List of Hydrocarbons That Are Not Measured or Not Reliably Measured by the HC1010 (Class b)

Class b hydrocarbon	k_{OH} at 298 K	Class a hydrocarbon used for interpolation	R^2
ethene	9.00×10^{-13}	benzene/cyclohexane	0.81
ethyne	8.52×10^{-12}	n-nonan	0.73
ethane	2.57×10^{-13}	benzene/cyclohexane	0.44
propene	2.63×10^{-11}	m/p-xylol	0.74
propane	1.12×10^{-12}	benzene/cyclohexane	0.85
2-methylpropane	2.19×10^{-12}	benzene/cyclohexane	0.96
1-butene	4.14×10^{-11}	ethylbenzene	0.55
1,3-butadiene	6.66×10^{-11}	ethylbenzene	0.01
n-butane	2.44×10^{-12}	benzene/cyclohexane	0.93
trans-2-butene	6.40×10^{-11}	ethylbenzene	0.01
cis-2-butene	5.64×10^{-11}	ethylbenzene	0.16
3-methyl-1-butene	3.18×10^{-11}	ethylbenzene	0.70
2-methylbutane	3.70×10^{-12}	3-methylpentane	0.88
1-pentene	3.14×10^{-11}	ethylbenzene	0.87
2-methyl-1-butene	6.10×10^{-11}	ethylbenzene	0.93
n-pentane	4.00×10^{-12}	3-methylpentane	0.92
cis-2-pentene	6.50×10^{-11}	ethylbenzene	0.31
2-methyl-2-butene	8.69×10^{-11}	ethylbenzene	0.52
cyclopentene	6.70×10^{-11}	ethylbenzene	0.01
1-hexene	3.70×10^{-11}	ethylbenzene	0.61
n-hexane	5.45×10^{-12}	3-methylpentane	0.96
cis-3-hexene	5.90×10^{-11}	ethylbenzene	0.26
trans-2-hexene	6.60×10^{-11}	ethylbenzene	0.40
2-methylhexane	5.10×10^{-12}	3-methylpentane	0.97
2,3-dimethylpentane	6.10×10^{-12}	3-methylpentane	0.95
2,2,4-trimethylpentane	3.57×10^{-12}	3-methylpentane	0.97
n-heptane	7.02×10^{-12}	n-nonane	0.90
3-methylheptane	8.56×10^{-12}	n-nonane	0.93
n-octane	8.72×10^{-12}	n-nonane	0.66
i-propylbenzene	6.6×10^{-12}	toluene/2/4-methylheptane	0.83
n-propylbenzene	5.7×10^{-12}	toluene/2/4-methylheptane	0.91

The third column shows those hydrocarbons (from class a) that were used as proxy for the interpolation. Rate coefficients are taken from *Atkinson* [1997] for alkanes and alkenes and from *Atkinson* [1994] for aromatics and ethyne. R^2: correlation of hydrocarbons from class b with class a as determined from the HP-GC data of 20 and 21 July.

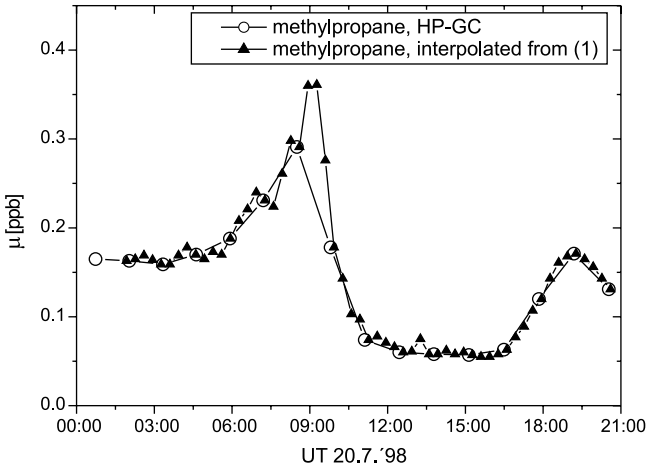

Figure 5. Original HP-GC data (open circles) and interpolated data (triangles) for methylpropane on 20 July. Toluene was used as proxy for the interpolation.

giving faith to the applicability of the interpolation procedure. The weaker correlation observed for alkenes is mostly due to their low mixing ratios.

[21] Figure 5 shows the diurnal variation of the original and the interpolated methylpropane mixing ratios on 20 July. The peak concentration of the interpolated data coincide with the maximum NO_x concentration in Figure 4. For verification of the procedure, hydrocarbons from class a) (ethylbenzene, m/p-xylene, and o-xylene) were interpolated in the same way and compared to the original data. Figure 6 displays the ratio of interpolated to original data as a function of the measured mixing ratio. Also shown is the uncertainty of the hydrocarbon measurements as estimated by *Konrad and Volz-Thomas* [2000] from simultaneous measurements made with the two GC systems. At lower mixing ratios, the scatter introduced by the interpolation procedure is not significantly larger than the scatter for simultaneous measurements [*Konrad and Volz-Thomas*, 2000]: About 72% of the data fall between the $\pm 1\sigma$ lines and 89% between the $\pm 2\sigma$ lines. At mixing ratios >100 ppt, the scatter of the data in Figure 6 is explained by an additional error of 5–10% arising from the interpolation procedure. This is significantly less than the potential errors arising from a linear interpolation of the HP-GC data, especially during the plume events (see Figure 5).

[22] The interpolated hydrocarbon data were used to characterize the observatory site during the first IOP. In Figure 7, the mixing ratios, the HC/NO_x ratio and the hydrocarbon reactivity toward OH are shown for all alkanes, alkenes (except isoprene and α-pinene), aromatics and the individual hydrocarbons ethyne, isoprene and α-pinene as a function of time in a stacked column diagram. The upper panel gives wind speed and direction (selected for WS > 0.5 m s^{-1}) and the toluene/benzene ratio. Although the hydrocarbon reactivity toward OH is shown for the whole time period, we should like to note that degradation

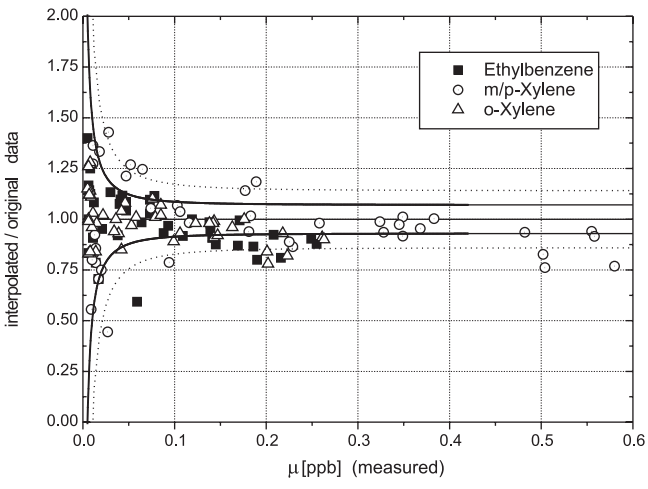

Figure 6. Ratio of interpolated to measured hydrocarbon concentrations as a function of the measured mixing ratio. The solid (1σ) and the dotted (2σ) curves correspond to the measuring uncertainty for hydrocarbons in ambient air (7% and 5 ppt) as estimated by *Konrad and Volz-Thomas* [2000].

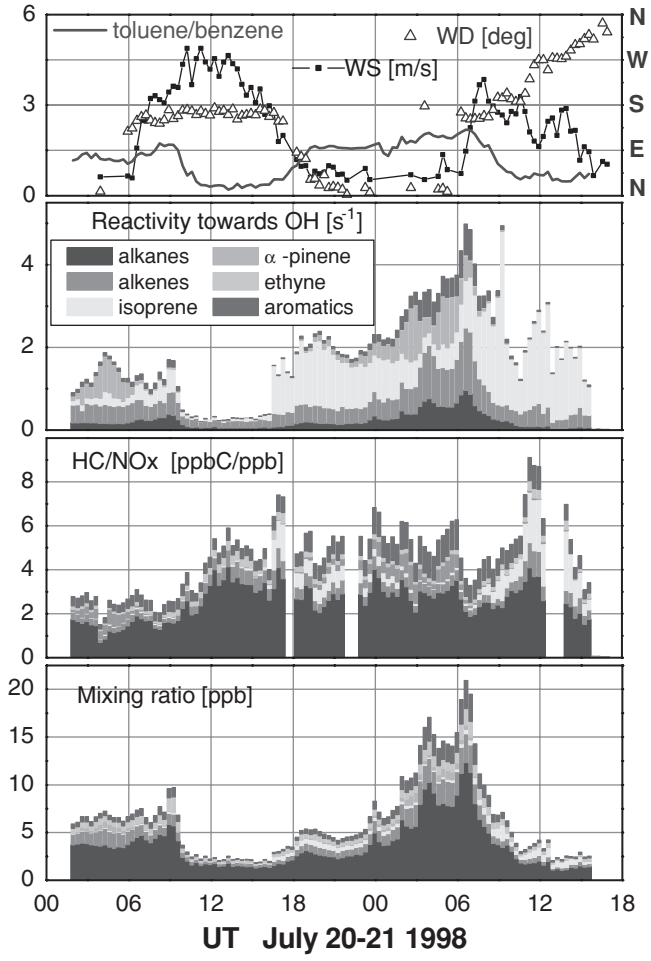

Figure 7. Time series of the hydrocarbon mixing ratios, the HC/NO_x ratio, and the HC reactivity toward OH at Pabstthum on 20 and 21 July adopted from the interpolated HC data. The hydrocarbons are subdivided into alkanes, alkenes, isoprene, α-pinene, ethyne, and aromatic compounds. The top panel gives the toluene/benzene ratio, wind speed (WS), and wind direction (WD). See color version of this figure at back of this issue.

of the hydrocarbons at night occurred mainly through reaction with NO_3 radicals [*Geyer et al.*, 2001], since the OH concentration usually declined below 0.5×10^6 mol cm^{-3} after sunset [*Holland et al.*, 2003].

[23] Alkanes were the most abundant hydrocarbon fraction during the whole IOP. They comprised ~60% on the basis of mixing ratios and a carbon atom basis (ppb C). Alkenes, aromatics and ethyne contributed approximately 23%, 9%, and 8% on the basis of mixing ratios, respectively. When considering the hydrocarbon reactivity toward OH on the other hand, alkanes contributed less than 20%, while the alkenes (including α-pinene and isoprene) comprised by far the largest fraction (>60%). Isoprene was the most important individual hydrocarbon concerning reactivity toward OH (on average: 40%). Within the time resolution of the GC (20 min) the largest fluctuation in the reactivity was also caused by isoprene. Examples are the sharp increase at 16 UT on 20 July and at 0916 UT on 21 July, which is not seen by the HP-GC due to its poor time resolution. Again, linear interpolation of the HP-GC data would lead to an underestimation of the total hydrocarbon reactivity by about a factor of 2. On a reactivity weighted basis, aromatic hydrocarbons comprised only 6%, on average, with somewhat higher amounts during the plume events (10% on 20 July and 15% on 21 July).

[24] The highest hydrocarbon concentrations on 20 and 21 July coincided with the highest NO_x values and the highest toluene/benzene ratios. The wind direction pointed at ~150°, e.g., to the western parts of Berlin and the city of Potsdam. At the same time the highest values of the NO_x/NO_y ratio were observed [*Volz-Thomas et al.*, 2003b]. The combination of all observations gives sufficient evidence that polluted air masses originating from the Berlin/Potsdam area were observed at Pabstthum. The sharp decrease of the hydrocarbon mixing ratios from 10 to 3 ppb at 0916 UT on 20 July, and the decrease of the toluene/benzene ratio from 1.6 to 0.5 coincides with a very slight change in wind direction from 150° to 155°–160°. Hence, it seems as if the observational site was located at the western edge of the plume on this day.

[25] The situation is quite similar on 21 July with the exception that the change in WD was more pronounced than on 20 July. Mixing ratios and hydrocarbon reactivity were a factor of 2 and 2.5 higher on 21 July, respectively. This has two reasons. As can be seen from the vertical soundings made at Pabstthum [*Glaser et al.*, 2003] the mixing layer height on 21 July at 7 UT was only 100 m, much lower than at 9 UT on 20 July (~800 m). Thus, the emissions were released into a much smaller volume than on 20 July. In addition, the plume was observed about 2 hours earlier in the morning. Therefore, chemical degradation of hydrocarbons should have been less pronounced than on 20 July. This point is supported from the toluene/benzene ratio, which reached a maximum of ~2.2 on 21 July, about 30% higher than on the day before. Given the extremely low wind speeds (<1 m s^{-1}) before 06 UT it seems unlikely that the maximum concentrations at 7 UT on 21 July were due to emissions from the city of Berlin. Because of the shallow boundary layer, emissions from minor sources closer to the site, such as the small villages Beetz or Kremmen (~8 and 14 km to the SW, respectively) [see map of *Volz-Thomas et al.*, 2003b] could have contributed to the precursor concentrations at Pabstthum in the morning of 21 July.

4. Discussion

[26] The hydrocarbon measurements were used together with the other trace gas measurements performed at Pabstthum to calculate the concentrations of the radicals OH, HO_2 and the sum of organic peroxy radicals (denoted RO_2) with the photochemical box model RACM [*Stockwell et al.*, 1997]. A few modifications were made in the model: The rate coefficients for the reaction of NO_2 with OH and HO_2 with NO were revised according to recent results by *Brown et al.* [1999] and *Bohn and Zetzsch* [1997], respectively. The photolysis frequencies JO^1D and JNO_2 were adopted from the filter radiometer measurements [*Holland et al.*, 2003; *Volz-Thomas et al.*, 2003b]. The other photolysis rates were calculated with the module PhotoRACM and then scaled with a constant factor that was determined from the ratio of the measured to calculated JNO_2 values.

[27] The chemical input parameters used for the simulations are listed in Table 2. In order to avoid over determination, the model was initialized with NO_x rather than with NO and NO_2. The VOCs were lumped on the basis of similarities in functional groups and reactivity according to *Stockwell et al.* [1997]. The average OH rate coefficient of each group (k_{OH}) was calculated from the relative contributions of the individual compounds to the group according to equation (1):

$$\bar{k}_{OH} = \frac{\Sigma k_{OHi} \cdot [VOC_i]}{\Sigma [VOC_i]} \quad (1)$$

RACM was initialized every 5 min with new input data. From the interpolated hydrocarbon data (time resolution of 20 min) data with a temporal resolution of 5 min were generated using the variation of NO_x during the respective 20 min interval:

$$\overline{[\mathrm{HC}]}_{5\mathrm{min}} = \frac{\overline{[NO_x]}_{5\mathrm{min}}}{\overline{[NO_x]}_{20\mathrm{min}}} \cdot \overline{[\mathrm{HC}]}_{20\mathrm{min}} \quad (2)$$

The concentrations of the diagnostic variables (OH, HO_2 and RO_2) and of those intermediates for which measurement were not available were initialized with zero. Since RACM is a time dependent model that cannot be operated in a steady state mode, the simulation in each 5 min interval was reiterated until the quasi steady state for the free radicals was established. In each iteration step, the measured concentrations were reset to the measured values and the radical concentrations were initialized with the output from the last iteration. Usually, the free radicals had approached steady state within 5% after three iterations.

[28] The results of the simulations are depicted in Figure 8 together with the measured OH and HO_2, and RO_2 concentrations [*Holland et al.*, 2003; *Mihelcic et al.*, 2003]. The measured NO_x mixing ratio, concentrations of condensation nuclei (CN) and JO^1D are shown in the lowest panel of Figure 8. Before 0930 UT, NO_x mixing ratios were >5 ppb (this period is denoted "high NO_x regime" in the following). After 10 UT NO_x mixing ratios dropped below 3 ppb, referred to as "low NO_x regime."

Table 2. Input Data for the Model Runs With RACM (n.m.: Not Measured)

Compound	RACM species	Measuring system
nitrogen monoxide	NO	CLD[a]
nitrogen dioxide	NO_2	CLD/PLC[a]
ozone	O_3	UV photometer[a]
nitric acid	HNO_3	Difference[a]
carbon monoxide	CO	NDIR[a]
methane	CH_4	n.m., 1.7 ppm
ethane	ETH	this work
ethene	ETE	this work
internal olefines	OLI	this work
terminal olefines	OLT	this work
isoprene	ISO	this work
HC with $k_{OH} < 3.4 \times 10^{-12}$	HC3	this work
HC with $3.4 \times 10^{-12} < k_{OH} < 6.8 \times 10^{-12}$	HC5	this work
HC with $k_{OH} > 6.8 \times 10^{-12}$	HC8	this work
toluene and less reactive aromatics	TOL	this work
xylenes and more reactive aromatics	XYL	this work
α-pinene and other cyclic terpenes with one double bond	API	this work
limonene and other cyclic diene terpenes	LIM	n.m., see text
acetaldehyde and higher aldehydes	ALD	DNPH GC/ECD
glyoxal	GLY	DNPH GC/ECD[b]
hydroxy ketones	HKET	DNPH GC/ECD[b]
methacrolein and other unsaturated monoaldehydes	MACR	DNPH GC/ECD[b]
methylglyoxal and other α-carbonyl aldehydes	MGLY	DNPH GC/ECD[b]
unsaturated dihydroxy dicarbonyl compounds	UDD	DNPH GC/ECD[b]
formaldehyde	HCHO	Hantzsch Monitor[b]
hydrogen peroxide	H_2O_2	HPLC, peroxidase[b]
peroxyacetyl nitrate	PAN	GC-ECD[a]
water vapor	H_2O	Psychrometer[a]
carbon dioxide	CO_2	n.m., 365 ppm
hydrogen	H_2	n.m., 500 ppt
oxygen	O_2	n.m., 20.1%
nitrogen	N_2	n.m., 78.1%
JO^1D, JNO_2		filter radiometer[a,c]
other J-values		PhotoRACM scaled by JNO_2

[a] *Volz-Thomas et al.* [2003b].
[b] *Grossmann et al.* [2003].
[c] *Holland et al.* [2003].

[29] In the high NO_x regime, the simulated concentrations of all three radicals agree with the measurements within the experimental errors. The importance of HONO photolysis for the radical budget in these air masses is discussed by *Alicke et al.* [2003]. The most important finding is that in the early morning (4–8 UT) when the high NO_x levels are encountered, the model predicts only 50% of the measured OH concentration, when HONO photolysis is switched off.

[30] In the low NO_x regime, simulated and measured RO2 concentrations continue to agree quite well. However, the OH and HO2 concentrations are overestimated by almost 100% and 40%, respectively.

[31] An important finding was that the NO_2/NO ratio predicted by RACM was, on average, 25% lower than the measured ratio. This finding is similar to the deviation of the measured NO_2/NO ratio observed to that calculated from the steady state of NO_x, JNO_2, O_3 and peroxy radicals as discussed by *Volz-Thomas et al.* [2003b]. These authors conclude that errors in the measurements are an unlikely explanation because of the excellent agreement between the CLD/PLC technique used for the measurement of NO_2 and NO with two independent spectroscopic methods (DOAS and MIESR) for NO_2. Therefore, the lower NO/NO_2 ratio gives evidence for an unknown oxidation reaction of NO to NO_2 in the atmosphere. A first order reaction of NO $\rightarrow$ NO_2 with a rate coefficient of $k_{NO \rightarrow NO_2} \approx 0.02\ s^{-1}$ was thus implemented in RACM in order to reproduce the measured NO/NO_2 ratio. The results are shown in Figure 9. We should like to note that other possibilities, such as a larger rate coefficient for the reaction of NO with all or at least a significant fraction of the peroxy radicals [cf. *Frost et al.*, 1998] could possibly explain some of the differences in the low NO_x regime. During early morning, however, when the peroxy radical concentrations are close to zero according to the measurements by MIESR, LIF, and chemical amplification, such an explanation would not change the NO/NO_2 ratio significantly (see also discussion by *Mihelcic et al.* [2003]). Most importantly, the analysis of the ozone budget from airborne measurements [*Corsmeier et al.*, 2002; *Volz-Thomas et al.*, 2003b] confirms the low ozone formation rates of 6–7 ppb hr^{-1} that are derived from the measured concentrations of NO, HO_2, and RO_2 with the currently accepted values for the rate coefficients.

[32] It is important to note that without correcting for the NO/NO_2 ratio, the modeled [OH] would be by 15% larger than the results shown in Figure 8, mainly because of less efficient recycling of OH from HO_2 and RO_2. The peroxy radical concentrations, on the other hand, remain basically unchanged. Although the additional NO $\rightarrow$ NO_2 conversion brings simulated and measured radical concentrations somewhat closer, the remaining difference between modeled and measured OH and HO_2 concentrations in the low NO_x regime is highly significant. Since the radical production in the model is tied to the measurements, a significant sink

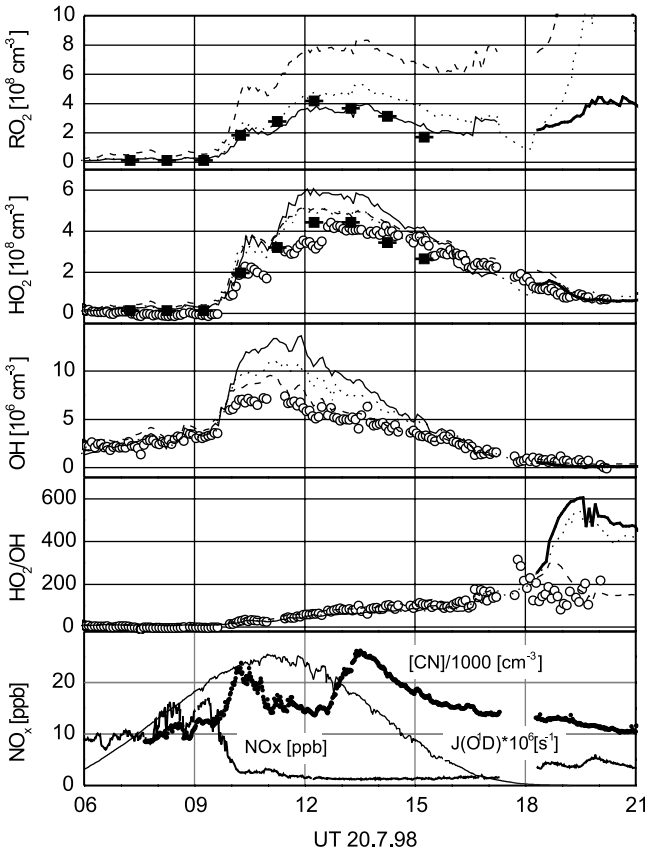

Figure 8. Diurnal variation of simulated and measured concentrations of free radicals (OH, HO_2, and the sum of all organic peroxy radicals RO_2) on 20 July at Pabstthum (open circles: LIF (OH and HO_2); squares: MIESR (HO_2 and RO_2); solid lines: RACM base case with additional NO → NO_2 conversion; broken lines: RACM with 500 ppt of limonene added). The dotted lines are results by *Mihelcic et al.* [2003] obtained with a chemical master mechanism. The lowest panel shows the NO_x mixing ratio, condensation nuclei (CN), and photolysis frequency $J(O^1D)$.

for HO_x radicals must exist in the atmosphere, which is not enclosed in the model's mechanism.

[33] In a number of studies [e.g., *Eisele et al.*, 1994, 1997; *Hauglustaine et al.*, 1999; *McKeen et al.*, 1997; *Perner et al.*, 1987; *Poppe et al.*, 1994; *Cantrell et al.*, 1996; *Savage et al.*, 2001] the observed [OH] was also overestimated by the models applied. Frequently, missing VOC reactivity was suggested as an explanation for the deviations between modeled and measured OH concentrations in the low NO_x regime. Since there is not enough NO present to convert all RO_2 radicals to HO_2, reactions among the peroxy radicals gain importance as the sink of HO_x. Therefore, HO_2 and OH radical concentrations are suppressed in model calculations with additional VOC reactivity in the low NO_x regime. In the high NO_x regime, on the other hand, additional VOC reactivity leads to enhancement of the radical concentrations [*Jeffries and Tonnesen*, 1994; *Kramp and Volz-Thomas*, 1997] since the reaction with hydrocarbons competes with the main HO_x sink, i.e., the reaction of OH with NO_2. In the first step, this leads to higher RO_2 concentrations, which are subsequently converted to HO_2 and OH. Additional HO_x is produced from the ozonolysis of alkenes [e.g., *Paulson and Orlando*, 1996].

[34] In order to test the influence of missing VOC reactivity on the radical concentrations at Pabstthum, 500 ppt of limonene were included in RACM as a surrogate of missing VOCs, thereby approximately doubling the reactivity represented by the measured hydrocarbons, oxygenated compounds, CO and methane in the low NO_x regime. The model calculations were conducted with the additional NO → NO_2 conversion. The resulting radical concentrations are also shown in Figure 8 (broken lines). As expected, the OH concentration increases by about 1×10^6 mol cm^{-3} in the high NO_x regime and is reduced by about 40% in the low NO_x regime. However, while OH and HO_2 are now in good agreement with the measurements, the RO_2 concentrations are almost a factor of 2 higher than the measurements by MIESR. Barring the highly unlikely speculation that a major fraction of the RO_2 radicals is not detected by MIESR [see *Mihelcic et al.*, 2003], the measurements made at Pabstthum clearly rule out missing VOCs as the major reason for the underestimation of OH by RACM at low NO_x concentrations.

[35] The simulated concentrations of all three radical species (OH, HO_2 and RO_2) can be brought into agreement with the measured values only if an additional loss reaction for HO_x is introduced into the model. When attributing the loss to a reaction of OH, a first order rate coefficient of approximately 1 s^{-1} would be required. If the losses were due to HO_2 reactions, the required rate coefficient would be about 50 times smaller. This result is similar to the steady state calculations by *Cantrell et al.* [1996], who proposed an unidentified OH sink that could be responsible for the model's overprediction.

[36] When introducing such a loss process into the model, an additional VOC reactivity equivalent to about 100 ppt limonene is necessary to bring measured and simulated RO_2 concentrations into accordance. Such a moderate amount of missing biogenic VOC reactivity

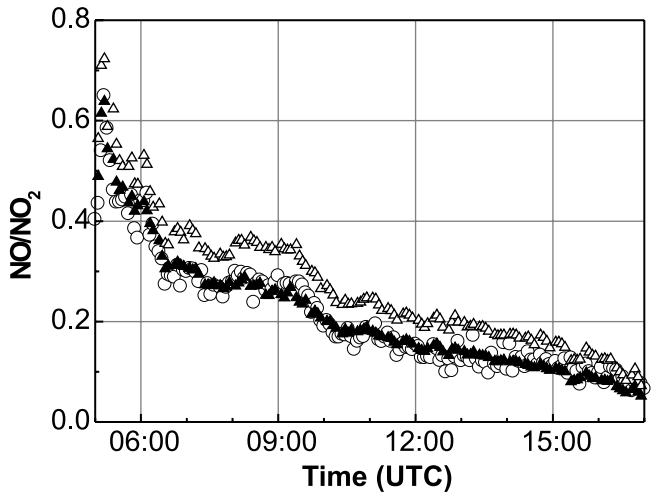

Figure 9. Measured NO/NO_2 ratios (open circles) as compared to the simulations with RACM with (filled triangles) and without (open triangles) additional NO → NO_2 conversion.

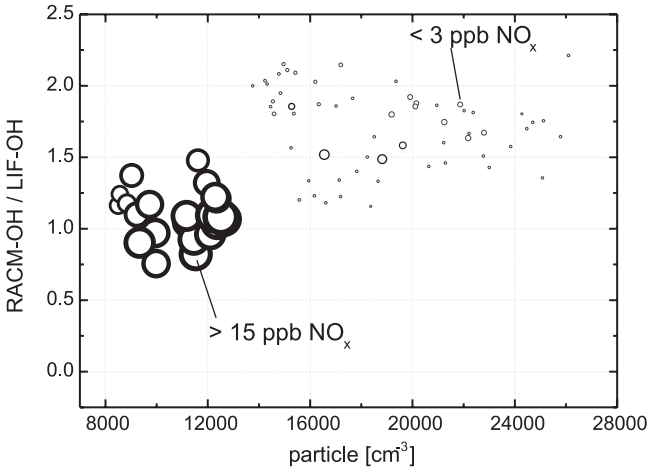

Figure 10. Ratio of simulated (with NO → NO_2 conversion, without additional limonene) to measured OH radical concentration versus the measured particle concentration on 20 July. The diameters of the symbols are proportional to the NO_x mixing ratio.

(20%) seems not unreasonable, since both GCs are not particularly optimized for the measurement of biogenic hydrocarbons. In particular, α-pinene was the only monoterpene detected on the HP-GC and tests of the inlet system after the campaign revealed the possibility for significant losses of α-pinene by up to 50%. It is, therefore, possible that biogenic monoterpenes were indeed underestimated at Pabstthum.

[37] *Mihelcic et al.* [2003] investigate the radical budget with the chemical master mechanism (MCM) of *Jenkin et al.* [1997]. The results are included in Figure 8 for comparison. The MCM predicts somewhat lower OH and HO_2 concentrations than RACM at low NO_x, most likely because of the more detailed description of the hydrocarbon oxidation mechanism including the formation of organic nitrates. However, the general finding for 20 July is similar with additional VOC reactivity leading to a significant overestimation of the RO_2 concentrations.

[38] A possible albeit speculative explanation for the missing HO_x sink is the loss on aerosol surfaces [*Cantrell et al.*, 1996], e.g., on organic aerosols that are build up during the oxidation of biogenic VOC [*Hoffmann*, 1999; *Hoffmann et al.*, 1997]. *Cantrell et al.* [1996] found much better agreement between measured and calculated HO_2 + RO_2 concentrations, when losses on aerosols were included based on the measured condensation nuclei concentrations and assuming a reaction probability per collision between 0.1 and 1. At Pabstthum, the atmospheric particle concentration was measured with a condensation nuclei counter. In Figure 10 the ratio of simulated to measured OH radical concentrations is shown as a function of the particle concentration. At a first glance, the model's overprediction of OH indeed seems to bare some correlation with the particle concentration ($R \sim 0.6$ for all data). However, this is mainly due to the different NO_x regimes and no correlation between the model's overprediction for OH and the particle concentration is observed at $NO_x < 3$ ppb. More information especially on the aerosol surface and its chemical composition is necessary for a deeper investigation of the impact of aerosol on HO_x concentrations.

[39] An interesting finding was the importance of PAN for the budget of the peroxy radicals, which was discovered incidentally due to a few missing data in the PAN measurements. The missing PAN concentrations were interpolated from the measurements for the model results shown in Figure 8. As shown in Figure 11 however, when PAN was initialized with zero instead of the 0.6–1 ppb measured on 20 July [*Volz-Thomas et al.*, 2003b], the RACM mechanism predicted significantly lower radical concentrations. The reduction was about a factor of 2 for the organic peroxy radicals with the largest contribution from CH_3O_2. The influence of PAN on HO_2 is still 20%, whereas OH is only decreased by a few percent, when PAN is neglected in the model. As the ozone production rate in the model is directly linked to the peroxy radical concentrations the results demonstrate the great importance of correct PAN data the for modeling of ozone episodes. The influence of the higher homologues of PAN should be of lesser importance, as their concentrations are around 10% or less of the PAN concentration [e.g., *Williams et al.*, 1993; *Roberts et al.*, 1998].

[40] We should also like to emphasize the uncertainty in the measurements of HCHO made at Pabstthum. As is discussed in more detail by *Grossmann et al.* [2003], the measurements made by DOAS gave almost a factor of 2 higher HCHO concentrations than the measurements made with the Hantzsch monitor, which were used in the model simulations presented here. *Mihelcic et al.* [2003] find approximately 20% larger HO_2 and 5–24% higher OH concentrations when the DOAS data are used for HCHO in the MCM calculations. Similar results are expected for RACM since HCHO is treated explicitly in the mechanism.

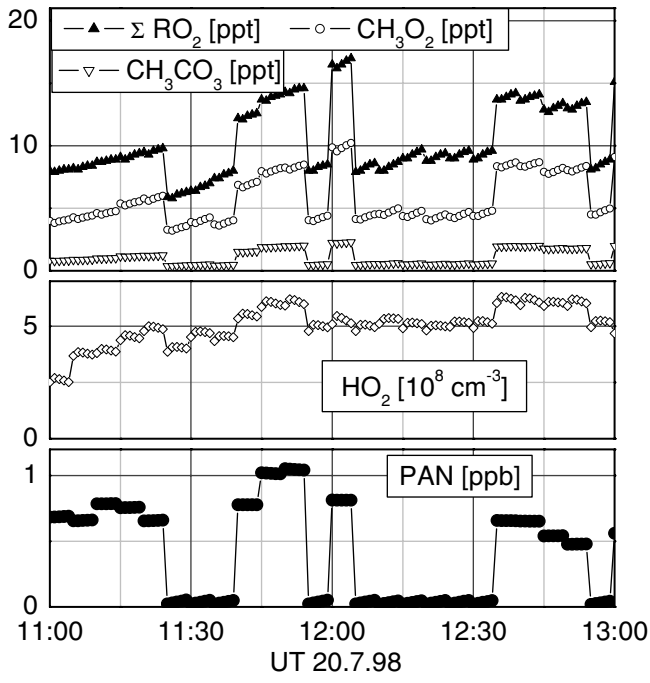

Figure 11. Influence of PAN (lower panel) on the simulated concentrations of organic peroxy radicals (upper) and HO_2 (middle).

[41] A minor point of uncertainty arises from the correction procedure for PhotoRACM described above. While this has no consequence for JNO_2 and JO^1D, where the actual measurements are used, it may influence the other J-values, which are corrected with the ratio of measured to calculated JNO_2. Comparison with the data from the spectral radiometer operated at Pabstthum [*Holland et al.*, 2003] reveals good agreement (within <5%) for most J-values, in particular JHCHO and JH_2O_2, whereas J_{HONO} is overestimated in the model by 20%. (Due to technical problems, the spectral radiometer produced data only for the morning of 20 July.) The consequence is a slight overestimation of the OH production rate in RACM during the early morning, e.g., in the high NO_x regime. Around noon, when the largest discrepancy is found between model and measurements, the influence of HONO photolysis on the HO_x concentration is only a few percent [cf. *Alicke et al.*, 2003].

5. Conclusions

[42] During summer 1998 measurements of atmospheric trace gases involved in the formation of photooxidants were performed about 50 km NW from the Berlin city center. The reactivity of the hydrocarbons toward OH was dominated by alkenes (>60%), in particular by isoprene and α-pinene. Air masses with the lowest photochemical age as estimated from the toluene/benzene ratio and the highest hydrocarbon and NO_x concentrations were observed on 20 and 21 July when air was advected from the direction of Berlin.

[43] By combining the hydrocarbon measurements performed with two GCs, a data set of more than 60 hydrocarbons from C_2 to C_{10} with a time resolution of 20 min was generated and used together with the other measurements performed at Pabstthum to predict OH, HO_2 and RO_2 concentrations with the photochemical box model RACM. Comparison with the measured radical concentrations shows relatively good agreement for NO_x mixing ratios >5 ppb. For lower NO_x mixing ratios, RACM overestimates the measured OH and HO_2 concentrations by up to 100% and 40%, respectively, similar to earlier investigations. Missing VOC reactivity, as often argued, is an unlikely explanation for the overestimation of HO_x, because the good agreement of measured and simulated RO_2 concentrations is lost when additional VOCs are included in the model. The overestimation of OH and HO_2 by the condensed RACM mechanism is more pronounced than by a chemical master mechanism. However, the much weaker dependence of the OH concentration on the NO_x concentration in the measurements than in current models points to a significant lack in our understanding of the atmospheric processes controlling the concentration of HO_x in unpolluted continental air.

[44] The model underestimates the measured NO_2/NO ratio by 25%. When letting the model find its own NO_2/NO ratio, the overestimation of OH and HO_2 becomes even more pronounced. The simulations also revealed the importance of PAN for the correct prediction of the peroxy radical concentrations and hence local ozone production rates.

[45] **Acknowledgments.** The work formed part of the first author's PhD thesis. The measurements were supported by the German Minister for Research and Development (BMBF) as part of the Tropospheric Research Focus (TFS) under grant no. 07TFS 31/HA.3. The authors are grateful to Heiner Geiß for implementing the RACM code at FZ-Jülich and for his helpful comments in the technical set up of the model calculations.

References

Alicke, B., A. Geyer, A. Hofzumahaus, F. Holland, S. Konrad, H.-W. Patz, A. Schafer, J. Stutz, A. Volz-Thomas, and I. Platt, OH formation by HONO photolysis during the BERLIOZ experiment, *J. Geophys. Res.*, *108*, doi:10.1029/2001JD000579, in press, 2003.

Atkinson, R., Gas-phase tropospheric chemistry of organic compounds, *J. Phys. Chem. Ref. Data Monogr.*, *2*, 216 pp., 1994.

Atkinson, R., Gas-phase tropospheric chemistry of volatile organic compounds, 1, Alkanes and alkenes, *J. Phys. Chem. Ref. Data Monogr.*, *2*, 215 pp., 1997.

Becker, K. H., B. Donner, and S. Gäb, BERLIOZ: A field experiment within the German Tropospheric Research Program (TFS), in *Proceedings of EUROTRAC Symposium 98 Vol. 2*, pp. 669–672, WIT Press, Southampton, 1999.

Blake, N. J., S. A. Penkett, K. C. Clemitshaw, P. Anwyl, P. Lightman, and A. R. W. Marsh, Estimates of atmospheric hydroxyl radical concentrations from the observed decay of many reactive hydrocarbons in well-defined urban plumes, *J. Geophys. Res.*, *98*, 2851–2864, 1993.

Bohn, B., and C. Zetzsch, Rate constants of a HO_2 + NO covering atmospheric conditions, 1, HO_2 formed by OH + H_2O_2, *J. Phys. Chem. A*, *101*, 1488–1493, 1997.

Brauers, T., M. Hausmann, A. Bister, A. Kraus, and H. P. Dorn, OH radicals in the boundary layer of the Atlantic Ocean, 1, Measurements by long-path laser absorption spectroscopy, *J. Geophys. Res.*, *106*, 7399–7414, 2001.

Brown, S. S., R. K. Talukdar, and A. R. Ravishankara, Rate constant for the reaction of OH + NO_2 + M → HNO_3 + M under atmospheric conditions, *Chem. Phys. Lett.*, *299*, 277–284, 1999.

Brandenburger, U., T. Brauers, H.-P. Dorn, M. Hausmann, and D. H. Ehhalt, In-situ measurement of tropospheric hydroxyl radicals by folded long-path laser absorption during the field campaign POPCORN in 1994, *J. Atmos. Chem.*, *31*, 181–204, 1998.

Cantrell, C. A., R. E. Shetter, T. M. Gilpin, J. G. Calvert, F. L. Eisele, and D. J. Tanner, Peroxy radical concentrations measured and calculated from trace gas measurements in the Mauna Loa Observatory Photochemistry Experiment 2, *J. Geophys. Res.*, *101*, 14,653–14,664, 1996.

Cantrell, C. A., R. E. Shetter, J. G. Calvert, F. L. Eisele, E. Williams, K. Baumann, W. H. Brune, P. S. Stephens, and J. H. Mather, Peroxy radicals from photostationary state deviations and steady state calculations during the Tropospheric OH Photochemistry Experiment at Idaho Hill, *J. Geophys. Res.*, *102*, 6369–6378, 1997.

Carpenter, L. J., P. S. Monks, I. E. Galbally, C. P. Meyer, B. J. Bandy, and S. A. Penkett, A study of peroxy radicals and ozone photochemistry at coastal sites in the Northern and Southern Hemisphere, *J. Geophys. Res.*, *102*, 25,417–25,427, 1997.

Carslaw, N., N. Bell, C. A. Lewis, J. B. McQuaid, and M. J. Pilling, A detailed case study of isoprene chemistry during the EASE96 Mace Head campaign, *Atmos. Environ.*, *34*, 2827–2836, 2000a.

Carslaw, N., P. J. Jacob, and M. J. Pilling, Understanding radical chemistry in the marine boundary layer, *Phys. Chem. Earth, Part C*, *25*, 235–243, 2000b.

Ciccioli, P., A. Cecinato, E. Brancaleoni, M. Frattoni, and A. Liberti, Use of carbon adsorption traps combined with high resolution gas chromatography: Mass spectrometry for the analysis of polar and non-polar C_4–C_{14} hydrocarbons involved in photochemical smog formation, *J. High Resolut. Chromatogr.*, *15*, 75–84, 1992.

Corsmeier, U., et al., Ozone and PAN formation inside and outside of the Berlin Plume—Process analysis and numerical process simulation, *J. Atmos. Chem.*, *42*, 289–321, 2002.

Ehhalt, D. H., Photooxidation of trace gases in the troposphere, *Phys. Chem. Chem. Phys.*, *1*, 5401–5408, 1999.

Eisele, F. L., G. H. Mount, F. C. Fehsenfeld, J. Harder, E. Marovich, D. D. Parrish, J. Roberts, and D. Tanner, Intercomparison of tropospheric OH and ancillary trace gas measurements at Fritz Peak Observatory, Colorado, *J. Geophys. Res.*, *99*, 18,605–18,626, 1994.

Eisele, F. L., D. J. Tanner, C. A. Cantrell, and J. G. Calvert, Measurements and steady state calculations of OH concentrations at Mauna Loa Observatory, *J. Geophys. Res.*, *101*, 14,665–14,680, 1996.

Eisele, F. L., G. H. Mount, D. Tanner, A. Jefferson, R. Shetter, J. W. Harder, and E. J. Williams, Understanding the production and interconversion of the hydroxyl radical during the Tropospheric OH Photochemistry Experiment, *J. Geophys. Res.*, *102*, 6457–6465, 1997.

Frost, G. J., et al., Photochemical ozone production in the rural southeastern United States during the 1990 Rural Oxidants in the Southern Environment (ROSE) program, *J. Geophys. Res.*, *103*, 22,491–22,508, 1998.

Geyer, A., B. Alicke, S. Konrad, T. Schmitz, J. Stutz, and U. Platt, Chemistry and oxidation capacity of the nitrate radical in the continental boundary layer near Berlin, *J. Geophys. Res.*, *106*(D8), 8013–8025, 2001.

Glaser, K., G. Baumbach, U. Vogt, A. Volz-Thomas, and H. Geiss, Vertical profiles of O_3, NO_2, NO_x, VOC, and meteorological parameters during the Berlin Ozone Experiment (BERLIOZ) campaign, *J. Geophys. Res.*, *108*, doi:10.1029/2002JD002475, in press, 2003.

Greenberg, J. P., P. R. Zimmerman, W. F. Pollock, R. A. Lueb, and R. E. Heidt, Diurnal variability of atmospheric methane, nonmethane hydrocarbons, and carbon monoxide at Mauna Loa, *J. Geophys. Res.*, *97*, 10,395–10,413, 1992.

Greenberg, J. P., D. Helmig, and P. R. Zimmerman, Seasonal measurements of nonmethane hydrocarbons and carbon monoxide at the Mauna Loa Observatory during the Mauna Loa Observatory Photochemistry Experiment 2, *J. Geophys. Res.*, *101*, 14,581–14,598, 1996.

Grob, K., and G. Grob, Gas–liquid chromatographic-mass spectrometric investigation of C6–C20 organic compounds in an urban atmosphere, *J. Chromatrogr.*, *62*, 1–13, 1971.

Grossmann, D., et al., Hydrogen peroxide, organic peroxides, carbonyl compounds and organic acids measured at Pabstthum during BERLIOZ, *J. Geophys. Res.*, *108*, doi:10.1029/2001JD001096, in press, 2003.

Habram, M., J. Slemr, and T. Welsch, Development of a dual capillary column GC method for the trace determination of C2–C9 hydrocarbons in ambient air, *J. High Resolut. Chromatogr.*, *21*, 209–214, 1998.

Hauglustaine, D. A., S. Madronich, B. A. Ridley, S. J. Flocke, C. A. Cantrell, F. L. Eisele, R. E. Shetter, D. J. Tanner, P. Ginoux, and E. Atlas, Photochemistry and budget of ozone during the Mauna Loa Observatory Photochemistry Experiment (MLOPEX 2), *J. Geophys. Res.*, *104*, 30,275–30,307, 1999.

Helmig, D., Ozone removal techniques in the sampling of atmospheric volatile organic trace gases, *Atmos. Environ.*, *31*, 361–3635, 1997.

Helmig, D., and J. P. Greenberg, Automated in situ gas chromatographic-mass spectrometric analysis of ppt level volatile organic trace gasses using multistage solid adsorbent trapping, *J. Chromatogr. A*, *677*, 123–132, 1994.

Hoffmann, T., Atmospheric chemistry of biogenic hydrocarbons: The contribution of vegetation to secondary organic aerosols, *EUROTRAC Newsl.*, *21*, 12–20, 1999.

Hoffmann, T., J. R. Odum, F. Bowman, D. Collins, D. Klockow, R. C. Flagan, and S. H. Seinfeld, Formation of organic aerosols from the oxidation of biogenic hydrocarbons, *J. Atmos. Chem.*, *26*, 189–222, 1997.

Holland, F., U. Aschmutat, M. Heßling, A. Hofzumahaus, and D. H. Ehhalt, Highly time resolved measurements of OH during POPCORN using laser-induced fluorescence spectroscopy, *J. Atmos. Chem.*, *31*, 205–225, 1998.

Holland, F., A. Hofzumahaus, J. Schäfer, A. Kraus, and H.-W. Pätz, Measurements of OH and HO_2 radical concentrations and photolysis frequencies during BERLIOZ, *J. Geophys. Res.*, *108*(D4), 8246, doi:10.1029/2001JD001393, in press, 2003.

Jeffries, H. E., and S. Tonnesen, A comparison of two photochemical reaction mechanisms using mass balance and process analysis, *Atmos. Environ.*, *28*, 2991–3003, 1994.

Jenkin, M. E., S. M. Saunder, and M. J. Pilling, The tropospheric degradation of volatile organic compounds: A protocol for mechanism development, *Atmos. Environ.*, *31*, 81–104, 1997.

Knobloch, T., A. Asperger, and W. Engewald, Volatile organic compounds in urban atmospheres: Long-term measurements of ambient air concentrations in differently loaded regions of Leipzig, *Fresenius J. Anal. Chem.*, *359*, 189–197, 1997.

Konrad, S., and A. Volz-Thomas, Characterization of a commercial gas chromatography-flame ionization detection system for the in situ determination of C5–C10 hydrocarbons in ambient air, *J. Chromatogr. A*, *878*, 215–234, 2000.

Koppmann, R., F. J. Johnen, A. Khedim, J. Rudolph, A. Wedel, and B. Wiards, The influence of ozone on light non methane hydrocarbons during cryogenic preconcentration, *J. Geophys. Res.*, *100*, 11,383–11,391, 1995.

Kramp, F., and A. Volz-Thomas, On the budget of OH radicals and ozone in an urban plume from the decay of C5–C8 hydrocarbons and NO_x, *J. Atmos. Chem.*, *28*, 263–282, 1997.

Lindinger, W., A. Hansel, and A. Jordan, On-line monitoring of volatile organic compounds at pptv levels by means of Proton-Transfer-Reaction Mass Spectrometry (PTR-MS) Medical applications, food control and environmental research, *Int. J. Mass Spectrom. Ion Processes*, *173*, 191–241, 1998.

McKeen, S. A., et al., , Photochemical modeling of hydroxyl and its relationship to other species during the Tropospheric OH Photochemistry Experiment, *J. Geophys. Res.*, *102*, 6467–6493, 1997.

Mihelcic, D., et al., Peroxy radicals during BERLIOZ at Pabstthum: Measurements, radical budgets, and ozone production, *J. Geophys. Res.*, *108*, doi:10.1029/2001JD001014, in press, 2003.

Mount, G. H., and E. J. Williams, An overview of the Tropospheric OH Photochemistry Experiment, Fritz Peak/Idaho Hill, Colorado, Fall 1993, *J. Geophys. Res.*, *102*, 6171–6186, 1997.

Paulson, S. E., and J. J. Orlando, The reactions of ozone with alkenes: An important source of HO_x in the boundary layer, *Geophys. Res. Lett.*, *23*, 3727–3730, 1996.

Penkett, S. A., P. S. Monks, L. J. Carpenter, K. C. Clemitshaw, G. P. Ayers, R. W. Gillet, I. E. Galbally, and C. P. Meyer, Relationships between ozone photolysis rates and radical concentrations in clean marine air over the Southern Ocean, *J. Geophys. Res.*, *102*, 12,805–12,817, 1997.

Perner, D., U. Platt, M. Trainer, G. Hübler, J. Drummond, W. Junkermann, J. Rudolph, B. Schubert, A. Volz, and D. H. Ehhalt, Measurements of tropospheric OH concentrations: A comparison of field data with model predictions, *J. Atmos. Chem.*, *5*, 185–216, 1987.

Poppe, D., et al., Comparison of measured OH concentrations with model calculations, *J. Geophys. Res.*, *99*, 16,633–16,642, 1994.

Roberts, J. M., et al., Measurements of PAN, PPN, and MPAN made during the 1994 and 1995 Nashville Intensives of the Southern Oxidant Study: Implications for regional ozone production from biogenic hydrocarbons, *J. Geophys. Res.*, *103*, 22,473–22,490, 1998.

Rudolph, J., The tropospheric distribution and budget of ethane, *J. Geophys. Res.*, *100*, 11,369–11,381, 1995.

Rudolph, J., F. J. Johnen, A. Khedim, and G. Pilwat, The use of automated "on-line" gas chromatography for the monitoring of organic trace gases in the atmosphere at low levels, *Int. J. Environ. Anal. Chem.*, *38*, 143–155, 1990a.

Rudolph, J., K. P. Müller, and R. Koppmann, Sampling of organic volatiles in the atmosphere at moderate and low pollution levels, *Anal. Chim. Acta*, *236*, 197–211, 1990b.

Savage, N. H., R. M. Harrison, P. S. Monks, and G. Salisbury, Steady-state modelling of hydroxyl radical concentrations at Mace Head during the EASE '97 campaign, May 1997, *Atmos. Environ.*, *35*, 515–524, 2001.

Schmitz, T., D. Klemp, and D. Kley, *Messungen der Immissions-konzentrationen verschiedener Ozonvorläufersubstanzen in Ballungsgebieten und an Autobahnen*, Forschung. Jülich, Jülich, 1997.

Schmitz, T., D. Hassel, and F.-J. Weber, Determination of VOC compounds in the exhaust of gasoline and diesel passenger cars, *Atmos. Environ.*, *34*, 4639–4647, 2000.

Stockwell, W. R., F. Kirchner, M. Kuhn, and S. Seefeld, A new mechanism for regional atmospheric chemistry modeling, *J. Geophys. Res.*, *102*, 25,847–25,879, 1997.

Trainer, M., E.-Y. Hsie, S. A. McKeen, R. Tallamraju, D. D. Parrish, and S. C. Liu, Impact of natural hydrocarbons on hydroxyl and peroxy radicals at a remote site, *J. Geophys. Res.*, *92*, 11,879–11,894, 1987.

Volz-Thomas, A., and B. Kolahgar, On the budget of hydroxyl radicals at Schauinsland during the Schauinsland Ozone Precursor Experiment (SLOPE96), *J. Geophys. Res.*, *105*, 1611–1622, 2000.

Volz-Thomas, A., J. Slemr, S. Konrad, T. Schmitz, and V. A. Mohnen, Quality assurance of hydrocarbon measurements in the German Tropospheric Research Focus (TFS), *J. Atmos. Chem.*, *42*, 255–279, 2002.

Volz-Thomas, A., H. Geiss, A. Hofzumahaus, and K.-H. Becker, The Fast Photochemistry Experiment in BERLIOZ (PHOEBE): An introduction, *J. Geophys. Res.*, *108*, doi:10.1029/2001JD002029, in press, 2003a.

Volz-Thomas, A., H.-W. Pätz, N. Houben, S. Konrad, D. Mihelcic, T. Klüpfel, and D. Perner, Inorganic trace gases and peroxy radicals during BERLIOZ at Pabstthum: An investigation of the photo stationary state of NO_x and O_3, *J. Geophys. Res.*, *108*, doi:10.1029/2001JD001255, in press, 2003b.

Wedel, A., K. P. Müller, M. Ratte, and J. Rudolph, Measurements of volatile organic compounds (VOC) during Popcorn 1994: Applying a new on-line GC-MS-technique, *J. Atmos. Chem.*, *31*, 73–103, 1998.

Williams, E. J., E. Grosjean, and D. Grosjean, Ambient levels of the peroxyacylnitrates PAN, PPN and MPAN in Atlanta GA, *J. Air Waste Manage. Assoc.*, *43*, 873–879, 1993.

K. Bächmann and S. Schlomski, Fachbereich 7: Chemie, Technische Hochschule Darmstadt, Germany.

H.-J. Buers, A. Hofzumahaus, F. Holland, N. Houben, S. Konrad, K. Mannschreck, D. Mihelcic, P. Müsgen, H.-W. Pätz, H.-J. Schäfer, Th. Schmitz, S. Schröder, and A. Volz-Thomas, Institut für Chemie und Dynamik der Geosphäre II, Forschungszentrum Jülich, D-52425 Jülich, Germany. (a.volz-thomas@fz-juelich.de)

D. Großmann and G. Moortgat, Division of Atmospheric Chemistry, Max-Planck-Institut für Chemie, Mainz, Germany.

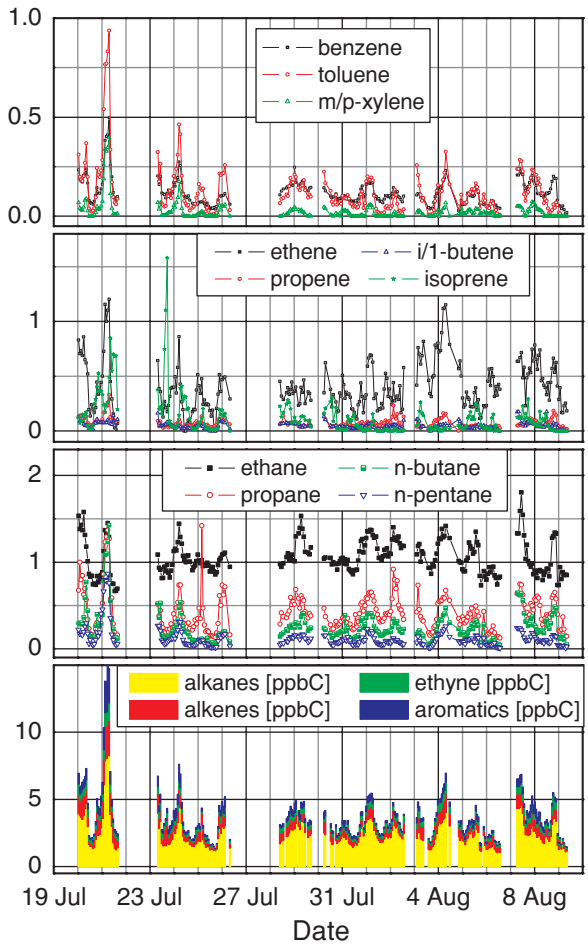

Figure 3. Time series of selected hydrocarbons as measured with the HP-GC at Pabstthum during BERLIOZ. The lowest panel shows the sum of all identified compounds and the breakdown into classes. The upper panels show the most abundant compounds of each hydrocarbon class.

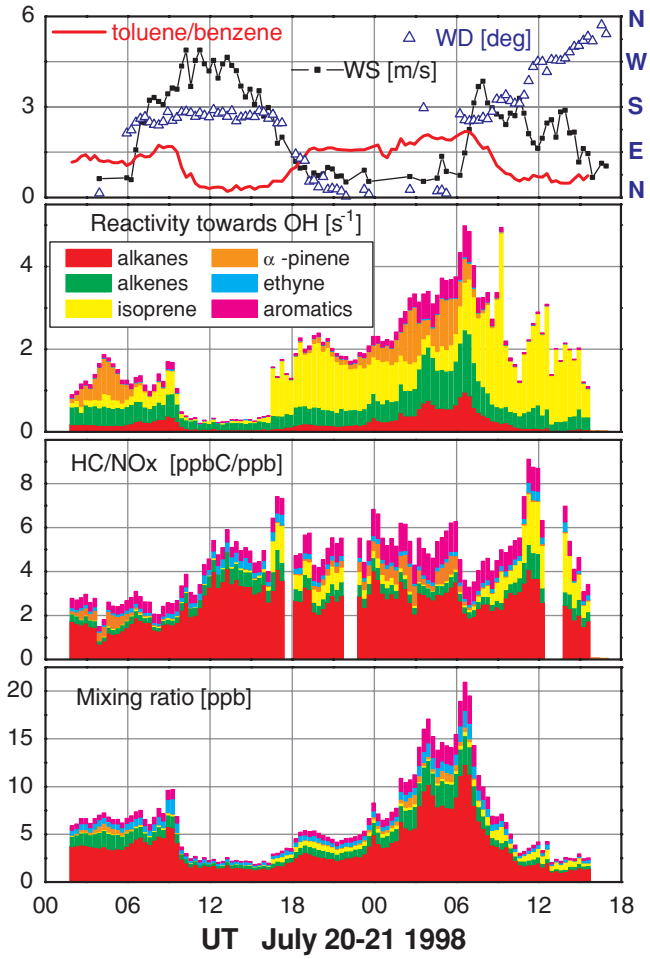

Figure 7. Time series of the hydrocarbon mixing ratios, the HC/NO_x ratio, and the HC reactivity toward OH at Pabstthum on 20 and 21 July adopted from the interpolated HC data. The hydrocarbons are subdivided into alkanes, alkenes, isoprene, α-pinene, ethyne, and aromatic compounds. The top panel gives the toluene/benzene ratio, wind speed (WS), and wind direction (WD).